15th International Congress on the Chemistry of Cement
Prague, Czech Republic, September 16-20, 2019

Reaction kinetics, reaction products and strength development of alkali-activated slag/fly-ash blends: Influence of activators

Siva uppalapati[a], Özlem Cizer[b]

Building Materials and Building Technology Division, KU Leuven, Heverlee, Belgium

[a]siva.uppalapati@kuleuven.be
[b]Ozlem.Cizer@bwk.kuleuven.be

ABSTRACT

This study investigates the influence of both the nature and concentration of alkaline solution on the reaction kinetics, hydration products and strength development of alkali-activated slag/fly-ash blends systems. Isothermal calorimetry was used to study the reaction kinetics of slag/fly-ash blends activated with three different alkaline solutions: sodium silicate, sodium carbonate and sodium sulfate. The results shown that the increase in alkali content (Na2O) leads to higher degree of hydration, while in the presence of CO32- and SO42- ions in solution, the rate of hydration decreases. The results show that the acceleration and strength development mainly depends on the nature of anions in activator rather than the alkalinity.

1. INTRODUTION

Alkali-activated materials (AAM) have been studied as a promising alternative to Portland cement for the development of more durable, sustainable and low-carbon construction and building materials with reduced environmental footprints [Pacheco. F et al., 2015, Provis. L et al., 2014]. In addition to its eco-friendly nature, AAM can also offer superior engineering properties like low hydration heat, high strength development, and excellent resistance against fire and chemical attacks [Provis. L et al., 2014, Shi. C et al. 2006]. Based on the chemical composition of the source material, AAM can be divided into two systems, including high-calcium system (alkali-activated slag) and low-calcium system (alkali-activation of fly-ash or metakaolin) [Pacheco. F et al., 2015, Provis. L et al. 2014]. The primary reaction product of alkali-activated slag (AAS) is C-S-H with Al in its composition [Jose. I et al., 2003], whereas the alkali-activation of fly-ash results in the formation of three-dimensional aluminosilicate networks via poly-condensation [John. L et al., 2014]. Recently, co-activation of calcium-rich slag and aluminosilicate-rich fly-ash have attracted increasing attention, as it counterbalances the critical drawbacks of each sole systems like quick setting, low mechanical strength, and high-volume instability [Gao. X 2017]. The reaction products in this system is highly depends on the calcium content and alkalinity of solution, but it is believed to induce coexistence of C-A-S-H and aluminosilicate gel (N-A-S-H) with higher degree of cross links [Puertas et al., 2000, Ismail et al., 2014].

Many researchers have identified that both the nature and dosage of activator are the main parameters involve in reaction process of alkali-activated materials (Huanhai et al., 1993, Buchwald. A et al., 2009, Ravikumar.D et al., 2012). Bernal. S et al., 2011 studies the influence of sodium oxide and silica-modulus on the AASF systems and reveals that increase in sodium oxide content and/or decrease in silica-modulus increases the rate of reaction and strength development. Although, the sodium silicate activator shows the comparable properties with OPC, their production process is quite energy intensive. Therefore, recently an environmentally friendly alkali sources like sodium carbonate and sodium sulfate have gain attention in alkali-activated materials. It has been shown that building made with sodium carbonate (Xu et al., 2008) and sodium sulfate (Anja. B et al., 2015) have accepted the strength and excellent in-suit performance. However, compared to sodium silicate activation, the reaction process of slag/fly-ash blends activated with sodium carbonate and sodium sulfate is less extensively studies by researcher and remains as the crucial research gap in literature.

This paper investigates the effect of nature and dosage of activator on the reaction kinetics, initial setting time, strength development and reaction products formation in AASF systems. The reaction process is indirectly studied using isothermal calorimeter, which enables the observation of heat flow associated with the overall chemical reaction and thermogravimetric analysis (TGA). The correlation between the reaction degree and strength development is elaborated. The influence of activator type and concentration on reaction products is investigated using X-ray diffraction.

2. EXPERIMENTAL PROGRAM

2.1 Materials and mix proportion

The Ground Granulated Blast Furnace Slag with a specific gravity of 2.92 g/cm^3 and Class-F Fly-ash with a specific gravity of 2.32 g/cm^3 were used as the primary materials in this study. The chemical composition of both slag and fly-ash, determined from X-ray fluorescence (XRF) spectrometry were given in Table 1.

Table 1: Chemical composition (by mass %) of slag and fly-ash.

Materials	SiO_2	Al_2O_3	Fe_2O_3	CaO	MgO	SO_3	MnO	K_2O
Slag	36.190	12.410	0.600	39.80	7.250	-	0.320	0.490
Fly-ash	57.440	26.130	6.290	2.43	1.49	0.830	0.052	2.900
Materials	**TiO_2**	**V_2O_5**	**SrO**	**ZrO_2**	**Cr_2O_3**	**S**	**BaO**	**Na_2O**
Slag	1.070	0.019	0.092	0.049	-	1.530	0.066	-
Fly-ash	1.340	0.048	0.135	0.050	0.018	-	0.138	0.450

Six different alkali-activated slag/fly-ash (AASF) binders were developed at 70:30 vol% of slag/fly-ash ratio by varying the type and concentration of activators as listed in Table 2. The alkaline solutions were prepared by dissolving solid sodium hydroxide, sodium carbonate and sodium sulfate in distilled water at least 24h before use. The prepared sodium hydroxide is mixed with commercially available sodium silicate (39-40% silicate in water) in order to achieve sodium metasilicate with a required alkali-modulus of 1.25 and 1.0. Simultaneously, prepared sodium carbonate and sodium sulfate were added to sodium metasilicare solution of alkali-modulus 1.0 in order to obtain molar ratios (SiO_2/Na_2O) of 0.7 and 0.6. Additional water was added to maintain the constant water-to-binder ratio at 0.5. The mortar samples with standard 1:3 binder to sand ratio were mixed according to EN 196-1 and cured at temperature of 20±1°C. River sand with a specific gravity of 2.60 g/cm^3 and water absorption of ≤0.5% is used as a fine aggregate. The paste samples were prepared using an overhead mixer at 750rpm for 2 min.

Table 2: Mixture proportion of Alkali-activated slag/fly-ash blends.

Mix ID	Activator Type	Modulus M_s= (SiO_2/Na_2O)	pH value
M1	Sodium Hydroxide + Sodium Silicate	1.25	13.65
M2	Sodium Hydroxide + Sodium Silicate	1.0	13.92
M3	Sodium Metasilicate + Sodium Carbonate	0.7	13.55
M4	Sodium Metasilicate + Sodium Carbonate	0.6	13.65
M5	Sodium Metasilicate + Sodium Sulfate	0.7	13.55
M6	Sodium Metasilicate + Sodium Sulfate	0.6	13.65

2.2 Experimental details

The workability of AASF mortars was investigated using flow table test according to the ASTM C230-14, where the diameter of the mortar spread in two directions at right angle is measured to calculated the flow value. Initial setting time of AASF paste samples were determined by means of standard Vicat Needle test method, according to EN 196-3: 2016. Standard mortar beams in 1:3 binder to sand ratio were tested for compression at 3, 7, and 28 days of curing respectively.

The reaction kinetics was investigated by using an isothermal conduction calorimetry (TAM Air device TA Instruments) up to 3 days at constant temperature of 20°C. The heat release was monitored on AASF paste samples (around 8-10g). Thermogravimetry (TGA) was performed using a Netzsch STA 409 PC DSC-TGA equipment in a through flow N_2 atmosphere over a temperature range of 30-650°C with a heating rate of 10°C/min. In this study, the weight losses between 30-650°C has been used as relative measure of the reaction degree in AASF. The analysis was performed on crushed samples at 3, 7, 28, 90, and 180 days after vacuum drying at 0.023 mbar for 2h to remove the free water.

X-ray diffraction (XRD, Bruker 2D PHASER) analysis is used to indicate which crystalline phases are formed at the age 7 days. X-ray diffraction patterns were collected in the 2θ range of 10 to 70^o with step size of 0.02^o and step time of 0.3s, and CuKα radition of 30 KV and 10 mA.

3. RESULTS

3.1 Workability

The flow values of slag/fly-ash blend activated with different type and concentration of activators are given in Table.3. The results indicates that the flow value of AASF mortars was influenced by both alkalinity and type of activator. The flow value decreased with the increase in the concentration of alkaline solutions or decrease in alkali-modulus. This can be attributed to the increase in viscosity of alkaline solution with the increase in concentration of activator. The samples activated with sodium silicate results low flow value compared to that of sodium carbonate and sodium sulfate activation, as sodium silicate is the most viscous solution.

Table 3: Flow values of AASF mortar samples.

Mix	M1	M2	M3	M4	M5	M6
Flow value [mm]	121	126	132	128	132	128

3.2 Heat of reaction

The heat evolution curves of slag/fly-ash blend activated with different type/concentration of activators were shown in Figure. 1. The heat evolution curves of AASF indicates two peaks: (1) an initial dissolution peak occurs within first few minutes, with a significant of heat release, and (2) an acceleration peak with relatively low intensity. The first dissolution peak can be attributed to the initial wetting/dissolution of source materials and formation of initial reaction complexes with dissolved Si and Al ions species. The acceleration peak corresponds to the precipitation of voluminous reaction products, both C-A-S-H and N-A-S-H gels. The peak valley in between first dissolution and second acceleration peak is called as induction period, which is associated with the precipitation of reaction products, formed with in first dissolution stage, on the surface on unreacted particles and temporarily hindering the reaction process. From Figure. 1, the duration of induction period seems to depend on both type and concentration of activator. The induction period of samples activated with sodium silicate is found to be shorter than the samples activated with sodium carbonate and sodium sulfate. The second acceleration peak of AASF becomes steeper and larger with increase in alkalinity of activators. This suggest that an increase in alkalinity enhances the dissolution of slag and increases the precipitation of reaction products. The area under the second acceleration peak is greater for the samples activated with sodium silicate, followed by sodium carbonate and sodium sulfate. This indicates that the three activators used followed this order with respect to the amount of reaction products formation: sodium silicate > sodium carbonate > sodium sulfate (major to minor).

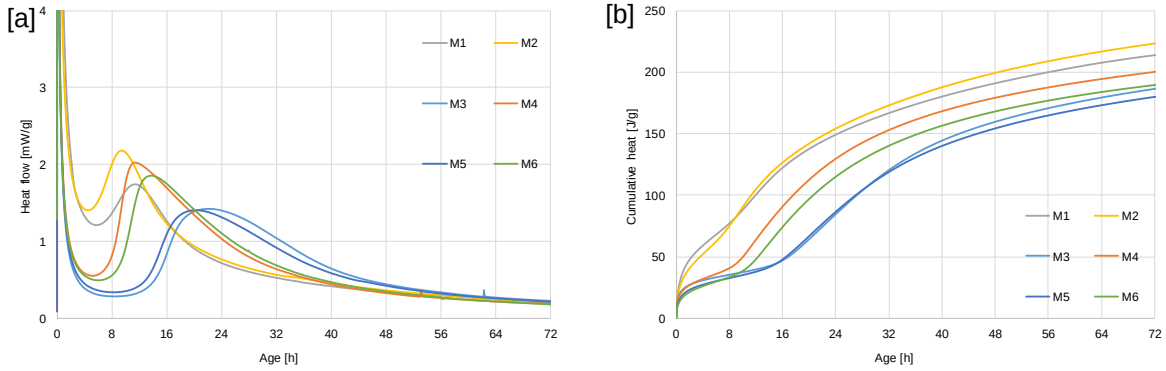


Figure 1. Heat evolution rate (a) and cumulative heat of reaction (b) of AASF samples.

The cumulative heat release, obtained by the integration of heat flow curves, is considered to be contributed by both the initial peak and secondary peak as shown in Figure. 1b. While the induction period is represented with a relative flatter region in between the initial rise and later rise of heat release. The cumulative heat release of AASF increases with an increase in alkalinity of activators, However, in samples (M1) activated with higher SiO_2 content resulted in higher heat release during first 7 hours. This may be due to the presence of addition aqueous silicates that contributes to the formation of more initial reaction complexes with dissolved alumina ion species.

3.2 Degree of reaction

In this section, an attempt is made to determine the degree of reaction (DoR) based on the heat release, which is supposed to be proportion to the overall chemical reaction of slag/fly-ash grains. The degree of reaction can be represented as the ratio of cumulative heat release Q(t) by the total heat release heat released at infinite time Q_∞ (Eq. 1). The main advantage of using heat release Q(t) is that it is a continuous measurement from the time of casting. However, the measuring of ultimate heat release Q_∞ from the isothermal calorimetry is virtually impossible as the accuracy of the heat flow is uncertain at this point. Therefore, an exponential model suggested by Freisleben-Hansen and Pedersen, FHP model (Pane & Hansen, 2002; Schindler & Folliard, 2005) is adopted to compute the ultimate heat release Q_∞

value, from the Eq. 2. Due to inability of this model for multi-curvature heat flow curves (observed two peaks in Figure. 1a), additional parameter (a_i) is applied for finding the ultimate heat release (Eq. 3).

$$\alpha(t) = \frac{Q(t)}{Q_\infty} \quad (1)$$

$$Q(t) = a_1 \exp\left(\left[\frac{-\tau_1}{t}\right]^{\beta_1}\right) + a_2 \exp\left(\left[\frac{-\tau_2}{t}\right]^{\beta_2}\right) \quad (2)$$

$$Q_\alpha = a_1 + a_2 \quad (3)$$

In the above exponential equation, τ and β are the time and shape parameters respectively. The FHP model fitting of the heat release curves are shown in Figure. 2.

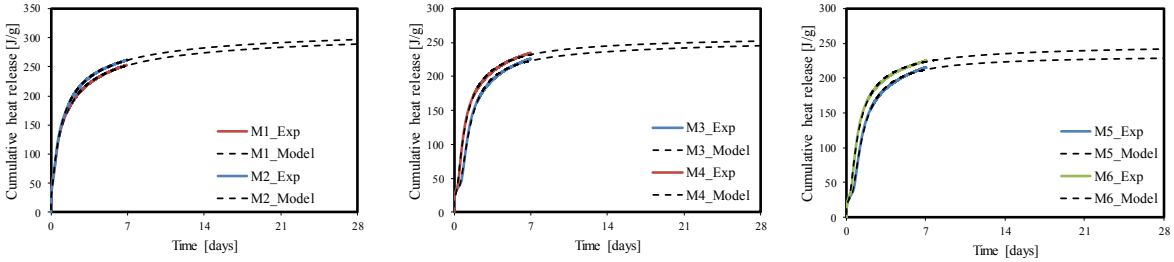


Figure 2. Exponential model fitting applied to the cumulative heat release of AASF pastes.

Figure. 3 presents the predicated degree of reaction for AASF pastes. It can be clearly seen that the reaction degree increases with increase in alkalinity, indicating that the reactivity of slag increases with increase in alkalinity. This is because the presence of OH^- ions enhances the degradation of slag particles and also increase the solubility of silicates and aluminate. As shown in Figure. 3, samples activated with sodium carbonate and sodium sulfate retarded the reaction at early-ages, as the presence of CO_3^{2-} and SO_4^{2-} ions reduces the alkalinity of solution. Once the CO_3^{2-} and SO_4^{2-} ions are exhausted, the reaction is accelerated and results in higher degree of reaction at later ages. The predicated reaction degree corresponded well with the measured isothermal calorimetry curves.

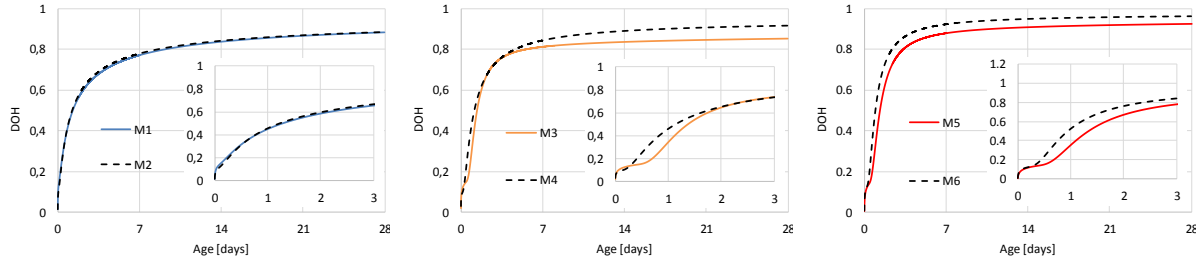


Figure 3. Reaction degree of slag/fly-ash blends activated with different alkaline solutions.

3.3 Thermogravimetry (TGA)

Table. 4 summaries the bound water content in AASF paste samples, calculate based on the weight loss between 30°C-650°C. It is apparent that the weight losses of AASF pastes increase with curing age. Samples activated with higher silica content (M1) shows lower bound water content during first 7-days and later shows higher bound water content compared to M2 samples. This is, on the one hand, because the addition silicates may suppresses the hydrolyzation rate of OH^- ions in the activator, leading to slower reaction at early-ages. Once silica ions are consumed in the formation of initial reaction products, the alkalinity of the solution starts rising and dissolves more ions and increase the rate of reaction. On the other hand, the reaction products formed with higher silica content (M1) may incorporates much more water than M2 samples having higher Na_2O content (M. Ben Haha et al 2011). An increase in alkalinity of sodium carbonate and sodium sulfate results higher bound water content. These results suggest that an increase in alkalinity of the activating solutions leads to more rapid dissolution of slag particles and increases the reaction products precipitation. Although, there is no significant difference in alkalinity of activators (M1, M4 and M6), the samples activated with sodium

silicate results higher chemical bound water than sodium carbonate and sodium sulfate. This indicates that the nature of anions in activator plays an important role in reaction rate of AASF systems.

Table 4: Bound water content of AASF pastes.

Mix	3 Days	7Days	28 Days	90 Days	180 Days
M1	11,940	13,861	16,745	17,247	17,806
M2	12,365	15,170	16,430	17,171	17,540
M3	9,974	11,658	13,897	13,948	15,688
M4	11,459	13.044	14.25	14,695	17,391
M5	9,293	10,654	12,620	13,252	14,896
M6	11,394	12,129	13,131	14,046	15,686

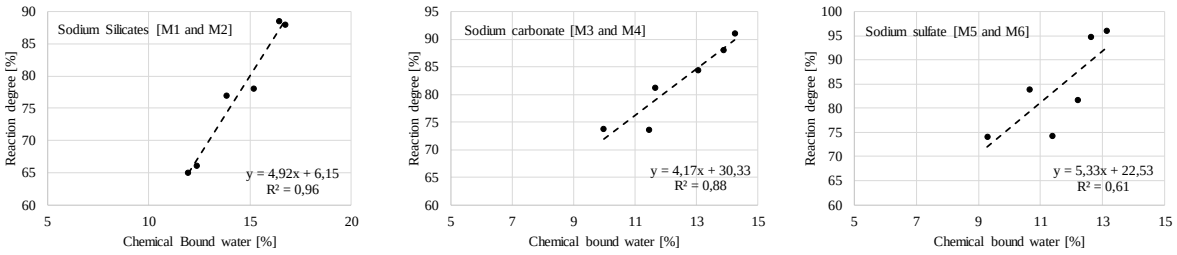


Figure 4. Correlation between the chemical bound water and reaction degree of AASF.

A correlation between the chemically bound water and the hydration degree of slag/fly-ash blend activated with different type of activators are given in Figure. 4. The reaction degree in relation with bound water content has a correlation close to linear in samples activated with sodium silicate. However, this correlation is weaker with addition of sodium carbonate and sodium sulfate, as shown in Figure. 4.

3.4 Initial setting time

The initial setting of slag/fly-ash blends activated with different type and concentration of alkaline solutions are summarized in Table. 5. As observed, the setting time is largely affected by nature activator. For example, the samples activated with a higher amount of SiO_2 results in shorter setting time and while with increase in CO_3^{2-} and SO_4^{2-} ions in activator results in an increase in setting time as shown in Table. 5. This is because, the presence of soluble silicates in activator readily react with the dissolved Ca^{2+} ions and forms more initial C-A-S-H gel. On the other hand, the presence of CO_3^{2-} and SO_4^{2-} ions may increases the time needed to saturate the ionic species required for the formation of reaction products, resulting setting.

Table 5: Initial setting time of alkali-activated slag/fly-ash blends.

Mix	M1	M2	M3	M4	M5	M6
Initial setting time [min]	40	50	65	80	70	90
Reaction degree [%]	9.1	8.8	9.1	8.9	8.5	9.1

Results shown in Table. 5 indicates that the reaction degree of 8.5 – 9.0 % corresponds to the formation of critical volume fraction of the hydration phases, resulting initial setting time. The formation of C-S-H gel is attributed to the initial reaction degree in sodium silicate activation. On the other hand, the formation of gaylussite and ettringite (see XRD results below), that do not have any influence on stiffening process, are considered to be the contribution of reaction degree at early-ages in samples

activated with sodium carbonate and sodium sulfate, respectively. This suggest that the formation of initial products is not critical for setting time in AASF pastes. In sodium silicate actiavtion, the monomeric and dimeric form of silicate species in alkaline solution reacts with dissolved aluminate ions from slag and fly-ash particles and rapidly form aluminosilicate structures and subsequently form C-A-S-H gel due to depolymerisation with dissolved calcium ions. While in sodium carbonate and sodium sulfate, the aluminosilicate structures are favoured at early-ages due to consumption of Ca^{2+} ion in the formation of gaylussite and ettringite, respectively. Therefore, irrespective of initial reaction products, the condensation reaction between the aluminosilicates units is more effectively leads to setting in AASF pastes.

3.5 Compressive strength

Figure. 5 shows the compressive strength of slag/fly-ash mortar blends activated with different alkaline solution described in table 2. It can be seen that the samples activated with a higher amount of SiO_2 (M1) resulted higher compressive strength at all ages. This is likely due to the formation of more hydrated C-A-S-H gel as result of higher concentration of admixed SiO_2 content. Samples activated with sodium carbonates shows lower compressive strength at early-age, as it forms gaylussite and hydroxysodalite, which does not give higher degree of cohesion necessary for developing the mechanical properties. However, the sodium carbonate activated samples results higher compressive strength at later ages due to the formation of carbonate compounds such as $C_3A.CaCO_3.12H_2O$ [Shao-Dong Wnag et al., 1994]. As shown in Figure. 5, samples activated with sodium sulfate exhibits lower strength at all ages. This is because of the formation of ettringite (see XRD) that may be causing a dispersive action between the hydrated products and coarsening of hydrated structure.

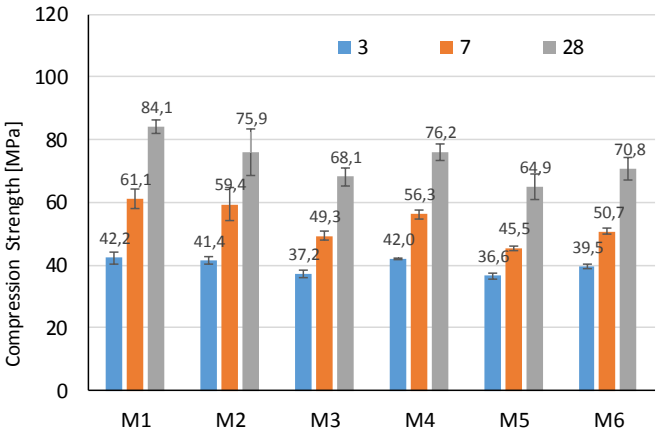


Figure 5. Compressive strength of slag/fly-ash mortar blend activated with different type and concentration of alkaline solutions.

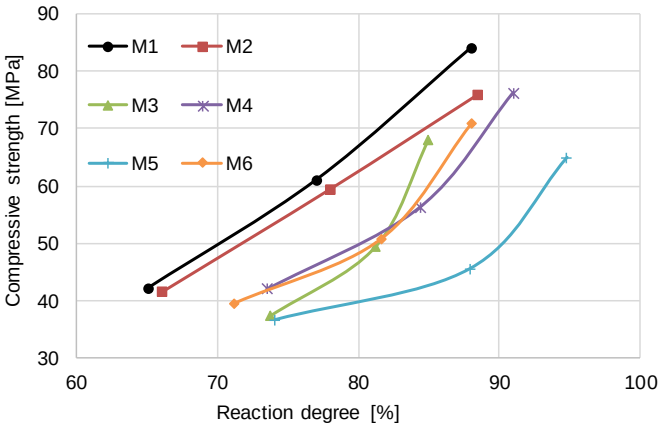
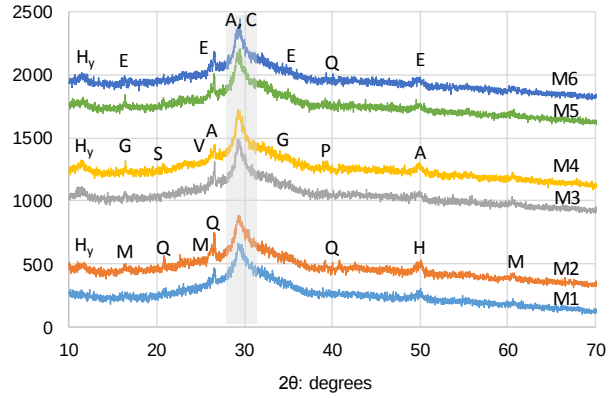


Figure 6. Correlation between the compressive strength and reaction degree of AASF.

Although the samples activated with alkali-modulus of 1.0 (M2) resulted in higher degree of reaction, the strength development is lower than the samples activated with alkali-modulus of 1.25 (M1) (Figure. 6). On the other hand, samples activated with sodium carbonate and sulfate also shows delay in strength development, even with the higher degree of reaction as shown in Figure. 6. This is likely due to the formation of gaylussite and ettringite instead of strength giving C-S-H phases. These results indicate that strength development is not only governed by volume of reaction products (degree of reaction) but also on the parameters like nature of reacted gel and/or pore structure.

3.6 X-ray diffraction

Figure. 7 shows the XRD patterns of the slag/fly ash blends activated with different alkaline solution at the age of 7 days. It can be seen that all mixes had a broad hump at about 2θ=29°, which can be attributed to the reflection of poorly crystalline C-A-S-H and/or N-A-S-H gels and could also be partly calcite from carbonation. Hydrotalcite ($Mg_6Al_2CO_3OH_{16}.4H_2O$) was detected as one of the main crystalline phases in all mixes. The peak intensity at about 2θ=13°, assigned to hydrotalcite increases with decrease in alkali-modulus as shown in Figure. 7. This is because, hydrotalcite, itself is a natural mineral, that forms at higher degree of reaction. In samples activated with sodium carbonate, unstable gaylussite ($Na_2Ca(CO_3)_2,5H_2O$) and hydroxysodalite ($Na_8Al_6Si_6O_24(OH)_2(H_2O)_2$) were observed as secondary reaction products as shown in Figure. 7. The formation of such phases at early-ages suggest that there is a preferential reaction between CO_3^{2-} and Ca^{2+} that dissolved from slag and forms gaylussite rather than C-S-H, which leads to saturation of silicon and aluminium species towards the formation of hydroxysodalite. Along with calcite, two polymorphs of calcium carbonate (vaterite and aragonite) and sodium–calcium carbonate phases (pirssonite) were observed in samples activated with sodium carbonate. Trace of ettringite is also observed in samples activated with sodium carbonate due to carbonation of mono-sulfate, formed due to presence of sulfate in slag. In samples activated with sodium sulfate, both ettringite and monosulfoaluminiate were observed as main secondary reaction products. In sodium sulfate activation, unreacted Na_2SO_4 in the form of thenardite is not identified as a crystalline phases, indicating that the most of sulfate has reacted with dissolved Al and Ca ions to form ettringite. Other phases like mullite, quartz, hematite, akermanite and gehlenite contributed to unreacted slag and fly-ash, were observed as shown in Figure. 7.



A – Amorphous: CASH and/or NASH

C – Calcite

H_y – Hydrotalcite ($Mg_6Al_2CO_3OH_{16}.4H_2O$)

G - Gaylussite ($Na_2Ca(CO_3)_2,5H_2O$)

S - Hydroxysodalite

E – Ettringite

Un-reacted phases:

M – Mullite; Q - Quartz; H - Hematite

Carbonate phases:

V – Vaterite; A – Aragonite; P - Pirssonite

Figure 6. XRD patterns of slag/fly-ash blends at the curing age of 7-days.

4. CONCLUSION

Based on the results and discussion following conclusion cans be drawn:

- The rate of reaction in AASF system is main influenced by the alkalinity of pore solution, and the nature of anion from activator could affect only at early-age reactions. With increase in alkalinity of alkaline solution, the heat of reaction increases. Addition of sodium carbonate and sodium sulfate results in longer induction period as the presence of CO_3^{2-} and SO_4^{2-} suppress the alkalinity of pore solution and rate of dissolution.

- The chemical bound water content increases with increase in alkalinity of sodium carbonate and sodium sulfate activators. While in sodium silicate activation, the samples with higher SiO_2

content or lower alkalinity results higher bound water content at later ages may be due to incorporates of more bound water in the reaction products.

- The setting time of AASF is largely affected by the nature of anion presence in alkaline solution. Samples activate with sodium sulfate results lower setting time and while in the presence of CO_3^{2-} and SO_4^{2-} ions the setting time is delayed. The reaction degree of 8.5-9% is corresponds to the initial setting time in AASF pastes.

- The compressive strength increases with higher silica content due to formation of more dense microstructure. With increase in alkalinity (Na_2O) content, the strength of sodium carbonate and sodium sulfate activated samples increases due to higher degree of reaction. Formation of gaylussite and ettringite reduces the strength development at early in samples activated with sodium carbonate and sodium sulfate, respectively.

- Both C-A-S-H and N-A-S-H gels are the primary reaction products in AASF samples activated with different alkaline solution. Hydrotalcite was found to be main secondary reaction product in sodium silicate activation. Additionally, to C-A-S-H and N-A-S-H gels, unstable phases like gaylussite were formed in samples activated with sodium carbonate at early-ages. Due to consumption of calcium ions in the formation of gaylussite, hydroxysodalite is favoured as a secondary phases. While in samples activated with sodium sulfate, ettringite is also formed as primary reaction products.

5. REFERENCES

Anja Buchwald, Maarten Vanooteghem, Elke Gruyaert, Harald Hilbig & Nele De Belie (2015). *Application of alkali-activated slag cement in Belgium in the 1950s*. Materials and structures, Volume 48, Issue1-2, pp 501-511.

Anja Buchwald., R. Tatarin., D. Stephan., (2009). *Reaction progress of alkaline-activated metakaolin-ground granulated blast furnace slag blends.,* Journal of Materials Science, Vol-44, Iss-20. PP. 5609-5617.

Deepak Ravikumar, Narayanan Neithalath., (2012). *Reaction kinetics in sodium silicate powder and liquid activated slag binders evaluated using isothermal calorimetry.,* Thermochimica Acta., Vol-546., PP-32-43.

Gao. X., (2017)., *Alkali activated slag-fly ash binders: design, modeling and application.,* PhD thesis., TU Eindhoven.

Huanhai, Zhou., Xuequan, Wu., Zhongzi, Xu., Mingshu, Tang., (1993), *Kinetic study on hydration of alkali-activated slag.,* Cement and Concrete Research, Vol-23, Issue 6, PP.1253-1258.

Ismail. I, S.A. Bernal, J.L. Provis, R. San Nicolas, S. Hamdan, J.S.J. van Deventer,. (2014). *Modification of phase evolution in alkali-activated blast furnace slag by the incorporation of fly ash,* Cem. Concr. Compos. 45 (2014) 125–135.

Jose I. Escalante-Garc, Antonio F. Fuentes, Alexander Gorokhovsky, Pedro E. Fraire-Luna, and Guillermo Mendoza-Suarez., (2003) *Hydration Products and Reactivity of Blast-Furnace Slag Activated by Various Alkalis.* J. Am. Ceram. Soc., 86 [12] 2148–53.

John L. Provis., (2014) *Geopolymers and other alkali activated materials: why, how, and what.* Materials and Structures, Vol -47, PP. 11–25.

M. Ben Haha, G. Le Saout, F. Winnefeld, B. Lothenbach (2011)., *Influence of activator type on hydration kinetics, hydrate assemblage andmicrostructural development of alkali activated blast-furnace slags*. Cement and Concrete Research, Vol 41, PP 301-303.

Pacheco T.F., Labrincha. A., Leonelli. C., Palomo. A., Chindaprasirt. P., (2015) Handbook of alkali-actiavted cements, mortars and concretes.

Pane, I. & Hansen, W., 2002. *Concrete Hydration and Mechanical Properties under Non isothermal Conditions*. ACI Materials Journal, 11, 99(6), pp. 534-542.

Provis. J, J.V. Deventer, Alkali activated materials, (2014) *State-of-the-art report, RILEM TC 224-AAM Springe Netherlands*.

Puertas. F, S. Martinez-Ramirez, S. Alonso, T. Vázquez,. (2000). *Alkali-activated fly ash/ slag cements: strength behaviour and hydration products,* Cem. Concr. Res. 30 (2000)

Schindler, A. K. & Folliard, K. J., 2005. *Heat of Hydration Models for Cementitious Materials*. ACI Materials Journal, Volume 102, pp. 24-33.

Shi. C., Krivenko. P.V., Roy .D.M., (2006). *Alkaline-activated cements and concretes*. Taylor and Francis, New York.

Shao-Dong Wang, Karen L. Scrivener and P.L. Pratt., (1994). *Factors affecting the strength of alkali-activated slag*., Cem. Concr. Res. Vol-24 1033-1043.

Susan A. Bernal, John L. Provis b, Volker Rose , Ruby Mejía de Gutierrez., (2011). *Evolution of binder structure in sodium silicate-activated slag-metakaolin blends.* Cement and Concrete Composites, Vol-33, Iss-1, PP-46-54.

Xu et al., 2008., H. Xu, J.L. Provis, J.S.J. Van Deventer, P.V. Krivenko., *Characterization of aged slag concretes.* ACI Mater. J., 102 (2008), pp. 131-139.